inter.noise
21-24 AUGUST
SCOTTISH EVENT CAMPUS
GLASGOW 2022

Modified acoustic black hole profile for improved fatigue performance

Archie Keys[1]
University of Southampton
SO17 1BJ, Southampton, United Kingdom

Jordan Cheer[2]
University of Southampton
SO17 1BJ, Southampton, United Kingdom

ABSTRACT

Acoustic black holes (ABHs) are realised via modifications to a structure that effectively reduce the structural wave speed; this increases the effect of damping treatments and thus enhances the achievable vibration attenuation. ABHs are commonly designed using a tapering thickness profile and this leads to part of the ABH being very thin. Due to the focusing effect of the ABH, the thin section of the taper is also exposed to high amplitude vibrations and this raises concerns relating the vibration fatigue of the structure. This paper investigates the fatigue life of an ABH taper used to terminate a beam using a numerical model, before a modified taper profile is proposed that aims to reduce the fatigue, while maintaining ABH performance. The effect of the power law used in the taper profile on the fatigue life is investigated and the potential trade-off between performance and fatigue life is explored for both the unmodified and modified profiles.

1. INTRODUCTION

Traditional techniques for passive vibration attenuation focus on the use of damping materials for the absorption of waves travelling through a structure, however, this has the drawback of increasing mass, as well as being limited to high frequencies where the wavelength is small relative to the damping treatment. Acoustic Black Holes (ABHs) are an alternative technique that allow for significant reductions in vibration amplitude across a larger frequency range, without increasing the mass of the structure. This is achieved by implementing modifications to the structure to effectively reduce the structural wavespeed, thus increasing the effectiveness of damping treatments.

The most common form of ABH is implemented using a power law taper that gradually decreases the thickness of a beam at its termination. This design was first proposed by Mironov [1], who presented a theoretical beam with a finite taper, ending in a zero thickness tip. The wavespeed along such a beam is proportional to the square root of its height and, therefore, the taper proposed by Mironov causes a wave approaching the tip of the beam to gradually slow down, such that it

[1]ak9g17@soton.ac.uk

[2]j.cheer@soton.ac.uk

would never reach the end due to the zero height at this point and the corresponding zero wavespeed. Therefore, in this theoretical case there would be zero reflection from the end of the beam.

In practice, it is not possible to manufacture a taper with zero tip height, and a power law tapering beam with a finite tip height leads to much of the incident wave being reflected back from the end of the taper. This issue can be resolved, however, by adding a thin, viscoelastic damping layer to the ABH taper, which acts to absorb the incident waves [2]. This damping layer is particularly effective since the decreasing thickness profile, which leads to a reduced wave speed within the taper and a reduced wavelength, gives more effective absorption.

The effectiveness of ABHs as a vibration attenuation solution has been thoroughly demonstrated [2–4], however, one outstanding issue lies in their strength. In order for an ABH to be effective it generally requires a very small tip height, resulting in a large portion of the taper being very thin. This has raised concerns about potential static failure of the structure if it is in a load bearing position, prompting alternative designs that reduce the stress in the material under static loading [5–7]. There has not, however, been a detailed analysis of the fatigue behaviour of an ABH. This is a concern due to the characteristic response of an ABH leading to a high amplitude of vibration at its thinnest part. Therefore, it is important that the vibration fatigue of ABHs is assessed, so that the potential failure can be predicted.

This paper presents a study into the fatigue life of a beam with a rectangular cross section, terminated with an ABH, before proposing a modified taper geometry based on an analytical function that aims to reduce fatigue while maintaining a low reflection coefficient. A 2D numerical model is used to examine the behaviour of the beam, quantifying the performance of the ABH in terms of both reflection coefficient and fatigue life for a range of power laws. This study provides insight into the vibration fatigue experienced by an ABH termination and this leads to the proposal of a modified taper geometry which is then optimised for fatigue and reflection coefficient. Section 2 describes how the numerical model used for this analysis was set up, before section 3 explains the performance metrics used to quantify both reflection and fatigue. Section 4 assesses the performance of an unmodified ABH in terms of reflection and fatigue, with both being explored for a range of power laws. Following this, Section 5 presents the modified taper profile, before comparing its performance to the unmodified ABH of the same power law. Section 6 summarises the work and draws conclusions based on the results.

2. NUMERICAL MODEL

To investigate vibration fatigue in ABHs, a 2D numerical model of a beam with a rectangular cross-section and an ABH termination was used, as shown in Fig. 1. This model allows both the reflection coefficient of the ABH and the fatigue life of the structure to be evaluated. This section outlines the set up of this model and explains how it has been used to obtain the results presented in Sections 4 & 5

The model geometry is comprised of a beam with rectangular cross-section and an ABH taper. The cross section dimensions are $b \times h(0)$ and the ABH taper has a height profile varying with distance along the beam, x, as follows:

$$h(x) = \left(\frac{l_{ABH} - x}{l_{ABH}}\right)^{\mu} (h_0 - h_{tip}) + h_{tip}, \tag{1}$$

where the origin of the x axis is at the junction of the beam and the ABH, l_{ABH} is the length of the ABH taper, μ is the power law with which the thickness of the structure decreases and h_{tip} is the finite height at the end of the ABH.

The model was implemented using the plate physics module in COMSOL, where a 2D geometry is built and then given a set thickness. As the third dimension this is defined as either the plate thickness, $h(0)$, or the ABH thickness defined by Equation 1. An input force was defined to act along the edge of

the non-ABH end of the beam, in the z direction with magnitude F, and the material used for both the ABH and the beam was aluminium alloy 6082-T6. The size of the mesh used in the model was chosen based on a mesh convergence study, which converged at approximately 4 elements per wavelength, which was calculated at 10 kHz and for the shortest wavelength, occurring at the tip of the taper.

The values of the parameters used to define the geometry of the model are shown in Table 1, which also shows the range of values used for the power law, *mu*, and the excitation force, F. Figure 1 shows the model geometry with the parameters labelled, including points x_1 and x_2 which are used to extract the reflection coefficient as described later in this section.

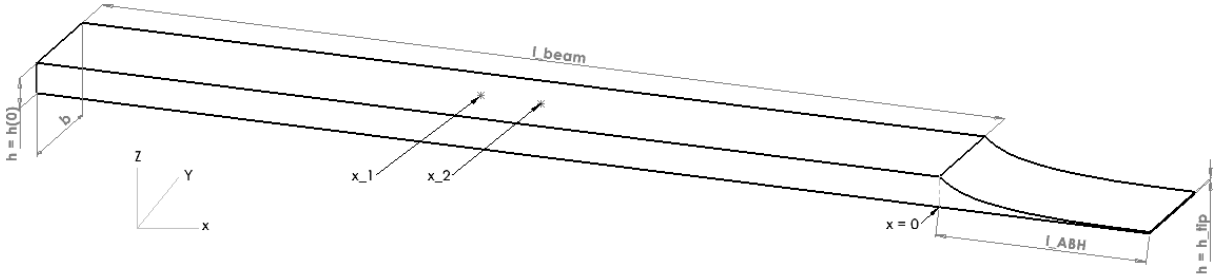

Figure 1: Beam with ABH termination: definition of geometric parameters.

Table 1: Parameter values as defined in figure 1.

Parameter	**Symbol**	**Value(range of values)**
Beam height	$h(0)$	10 mm
Beam length	l_{beam}	300 mm
Beam width	b	40 mm
ABH length	l_{ABH}	70 mm
ABH tip height	h_{tip}	0.6 mm
ABH power law	μ	4 (1-10)
Excitation force	F	80 N (0.8-80)

2.1. Damping

As noted in the introduction, a practical ABH requires damping material to be added to the taper and this is typically implemented using a thin, viscoelastic layer applied to one side of the ABH. The numerical model approximates this using an isotropic loss factor, with a value of 0.002 for the main beam section and 0.2 for the ABH section. Since the level of damping is dependent on both the isotropic loss factor and the volume of the structure, to ensure that the amount of damping being represented in the taper remains constant as its geometry is modified, the second damping value must be adjusted when comparing different taper geometries. The isotropic loss factor in the taper section is thus scaled based on the volume of the taper such that the total amount of damping in the ABH remains constant and is the same as that for a power law of 4 with a loss factor of 0.2. In practice, the viscoelastic damping layer applied to the taper will also add a distributed mass loading to the taper and this has been included in the 2D model by applying an additional mass of 11.9g, distributed across the ABH section.

3. PERFORMANCE METRICS

This paper aims to assess the performance of an ABH taper in terms of both its ability to attenuate vibrations and its fatigue life. The proposed modified taper aims to extend the fatigue life of the structure while maintaining ABH performance, therefore the performance in both of these areas must be quantified. Section 3 outlines the performance metrics used and how they are calculated from the modelled responses.

3.1. Reflection coefficient

The performance of beam-based ABHs is typically evaluated in terms of the reflection coefficient. The reflection coefficient can be calculated using the wave decomposition method described in [3]. This method uses the velocities evaluated or measured at two points on the beam to calculate the complex amplitudes of the positive and negative going waves as

$$\Phi^{+} = \frac{-1}{2\omega \sin\left(k_f \Delta_x\right)}\left[\dot{w}(x_1)e^{ik_f\Delta_x/2} - \dot{w}(x_2)e^{-ik_f\Delta_x/2}\right], \tag{2}$$

$$\Phi^{-} = \frac{-1}{2\omega \sin\left(k_f \Delta_x\right)}\left[\dot{w}(x_2)e^{ik_f\Delta_x/2} - \dot{w}(x_1)e^{-ik_f\Delta_x/2}\right], \tag{3}$$

where $\dot{w}(x)$ is the transverse velocity of the beam at point x, Φ^{+} and Φ^{-} are the complex amplitudes of the positive and negative going waves respectively, k_f is the flexural wavenumber in the beam section and Δ_x is the separation between the two points x_1 and x_2. The complex amplitudes of the positive and negative going waves can then be used to calculate the reflection coefficient as

$$|R| = \left|\frac{\Phi^{-}}{\Phi_{+}}\right|. \tag{4}$$

3.2. Fatigue

The fatigue performance of the ABH terminated beam is evaluated in terms of the 'fatigue usage factor', or f_{us}, which is a normalised fatigue measurement. A value of $f_{us} = 0$ means that the fatigue limit has not been exceeded and therefore no damage has been done to the structure, whereas a value of $f_{us} = 1$ means that the fatigue life of the material has been met, and a crack will have formed. It follows that a value of $0 < f_{us} < 1$ means that the component has experienced damage, but not yet reached its fatigue life, and a value of $f_{us} > 1$ means that the fatigue life has been exceeded. The fatigue usage factor is calculated using Equation 5 as

$$f_{us} = \sum_{p=1}^{q} \frac{n_p}{N_p}, \tag{5}$$

where q is the number of frequencies included in the fatigue calculation, n_p is the damage due to the pth frequency and N_p is the amount of damage required for the material to reach its fatigue life at the pth frequency [8]. The value for N_p is obtained from the $S - N$ curve for aluminium, which is defined within the model. The curve used here was obtained from [9], which explored various $S - N$ curves for aluminium, and defines the stress in MPa as

$$S = \left(10^{-b}N\right)^{1/m_w}, \tag{6}$$

where b and m_w are constants which were set as $b = 20.7$ and $m_w = -7.1$ based on [9].

In order to evaluate the fatigue usage factor, the modelled beam was excited by an input force acting along the edge of the non-ABH edge of the beam, as described in Section 2, with a time history defined by spending 0.5 s at each linearly spaced frequency point, ranging from 100 Hz to 10 kHz.

This results in a total of 201 frequency points and a total excitation time of 100.5 s, which means that the fatigue life of the structure can be calculated by dividing this excitation duration by the fatigue usage factor. The linear frequency spacing has been chosen to be consistent with a white noise force excitation, which represents a general vibration condition rather than an excitation condition that is relevant to a specific application.

4. CONVENTIONAL ABH POWER LAW

This section presents the results based on the conventional power law taper geometry using a range of power laws, starting with the reflection coefficient, before an initial assessment of fatigue life is presented.

4.1. ABH reflection performance

The numerical model was run across a frequency range of 100 Hz - 10 kHz with a step size of 49.5 Hz, using the parameters in Table 1. The reflection coefficient was calculated as outlined in section 3.1, before being averaged over frequency to provide a broadband measure of the ABH performance. This process was carried out for power laws of each integer value between 1 and 10, and the results are shown in Figure 2. The average reflection coefficient value is at a minimum for a power law of 4, and increases to higher values both above and below this point. This behaviour is well known and can be related to the trade off that is inherent with an acoustic black hole: a sharper taper will provide a more rapid decrease in the incoming wave speed, but will also cause an increasing proportion of the incident wave to be reflected from the junction between the ABH and the beam [10]. The best performance therefore occurs when these two behaviours are balanced.

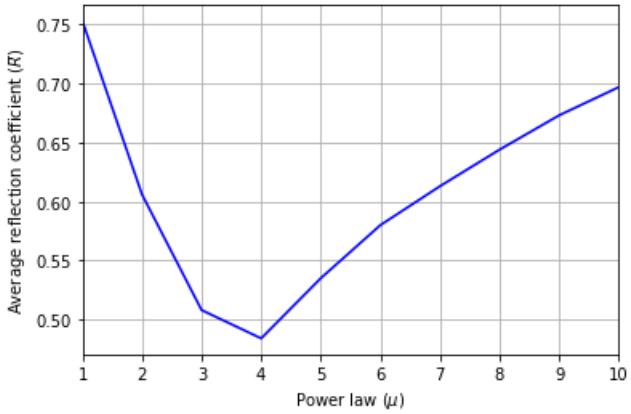

Figure 2: Average reflection coefficient, $\bar{R}$, for power laws from 1-10.

4.2. Fatigue analysis

Initially, an assessment of fatigue was carried out for a structure with the parameters listed in Table 1, for a power law of 4, allowing the fatigue life to be compared for a range of input forces between 0.8 and 80 N. This allows the magnitude of vibrational force needed to damage the structure to be assessed, helping to understand the significance of ABH fatigue. Figure 3 shows the resulting maximum fatigue usage factor and corresponding fatigue life for the ABH termination with a power law of 4 as the input force is varied. From the results is can be seen that a linear increase in force produces a logarithmic increase in the fatigue usage factor and a corresponding logarithmic decrease in fatigue life. This is expected, since stress is linked logarithmically to the fatigue life of a structure via the $S - N$ curve. It takes a significant amount of vibrational force to reduce the fatigue life sufficiently such that it would become significant for a component, meaning the fatigue life is shorter

than the expected life of the component. However, it is also important to consider the case of a variable amplitude load since most real world vibration sources will not generate a constant amplitude force, but will more likely vary over time and contain several discrete tones combined with some form of broadband random noise. It is more likely that a vibration fatigue-related failure will occur due to several, short-lived events where the input force is very high. For example, in this case it would take less than 3 minutes total time for the vibration force of 80 N to cause the structure to fail.

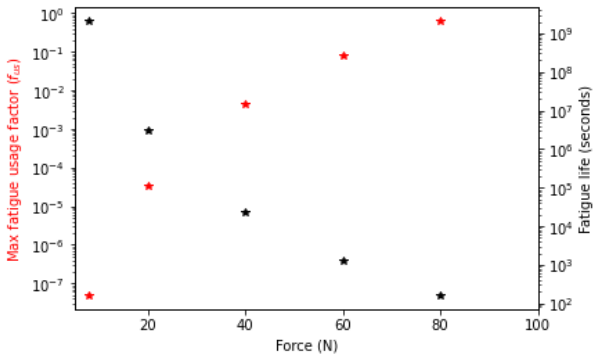

Figure 3: The maximum fatigue usage factor and fatigue life for a range of input forces

In order to assess the distribution of the potential damage across the surface of the ABH, a fatigue study was conducted on an ABH terminated beam with the parameters given in Table 1, for a power law of 4. The magnitude of the input force was set to 80 N acting along the edge of the beam, as detailed in Section 2, with a time history consisting of discrete frequency excitations of 0.5 s in length at 201 linearly spaced frequencies between 100 Hz and 10 kHz. The results of this study are shown in Figure 4, where it can be seen that the fatigue usage factor is highest within the ABH itself. The area of high fatigue is concentrated in a strip across the width of the taper, with higher levels occurring in regions to the edges of the structure. This is in agreement with the general vibration fatigue literature, which has found that concentrations of fatigue often occur at the edges of a structure [11].

The results present to this point have provided some insight into the vibration fatigue performance of a power law 4 ABH profile, however, it is also insightful to observe how the fatigue usage factor varies against the average reflection coefficient as the power law is varied from $1 - 10$, and this is presented in Figure 5. This plot allows the performance trade-off between fatigue and ABH performance to be visualised, with low values for both parameters being favourable. The black points represent the conventional ABH profiles, with the number beside each point corresponding to the power law used, and the point labelled with a power law of zero is for a beam without an ABH taper. Ideally an ABH would have a low reflection coefficient and a low fatigue usage factor, and therefore its data point would be located in the lower left of the plot. Conversely, power laws with data points in the upper right do not perform as well. In the following section, a modified ABH profile design in proposed, which utilises the insight into the ABH power law profile vibration fatigue performance that the results in this section have provided.

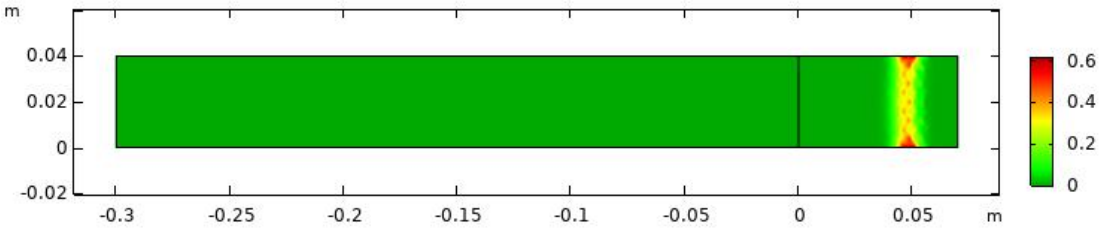

Figure 4: Fatigue usage factor across the surface of the beam and ABH for a power law of 4

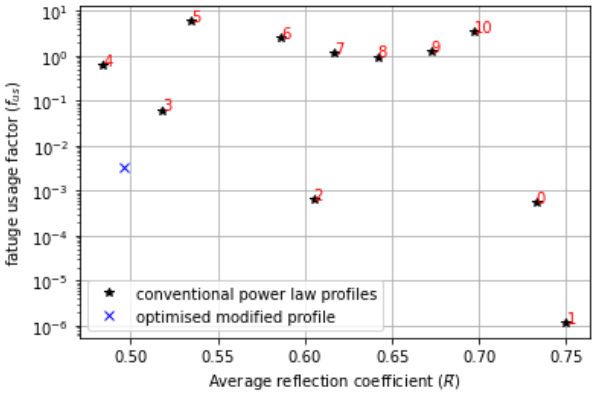

Figure 5: Fatigue usage factor versus average reflection coefficient for both the conventional ABH power law profile taper beam termination and the modified profile design. The conventional ABH tapers are labelled according to their power law, with zero indicating a beam without an ABH.

5. MODIFIED PROFILE

The results presented in the previous section suggest that vibration fatigue may limit the expected service life of an ABH terminated beam. In particular, Figure 4 shows that the fatigue concentrates in a strip across the width of the taper, with particularly high levels around the edges of the taper. This fatigue distribution is used to motivate a modified profile that aims to reduce the fatigue experienced within the ABH taper, while maintaining its reflection performance. The approach proposed here is to increase the thickness of the tapering termination in the areas of high fatigue, such that the stresses in these regions will be reduced and result in an extended fatigue life for the structure.

The modified profile is defined by multiplying the conventional power law height function, $h(x)$, by a multiplier, $M(x)$ to give $h_{mod} = h(x)M(x)$, where $M(x)$ is defined as

$$M(x) = -A\cos\left(\frac{\pi x^n}{l_{ABH}^n} - \frac{\pi}{2}\right)\cos\left(\frac{\pi y}{b} - \frac{\pi}{2}\right) + Am\cos\left(\frac{\pi x^n}{l_{ABH}^n} - \frac{\pi}{2}\right) + 1, \tag{7}$$

where A, n and m are scalar parameters. A allows the amplitude of the modifications to be changed, while n changes the position of the raised sections and m modifies the profile along the centre line of the ABH; when $m = 1$ the centre line of the ABH taper is unchanged by the function in an effort to preserve the reflection performance, but as m increases above 1 this part of the taper increases in thickness. Regardless of the parameter values used, the multiplier, $M(x)$, will be equal to 1 at both the beam-ABH junction and the ABH tip, such that the junction between the beam and taper is unchanged and the tip height is also maintained.

The parameters A, n and m have been optimised using an interior-point algorithm to minimise a weighted sum of the maximum fatigue usage factor and the broadband averaged reflection coefficient. The resulting cost function was defined as

$$J = \bar{R} + a \times \log_{10}(f_{us,max} \times 10^6), \tag{8}$$

where a is a scaling factor used to adjust the relative importance of minimising the broadband averaged reflection coefficient and the maximum fatigue usage factor. The fatigue usage factor is scaled logarithmically so that a linear decrease in the cost function corresponds to a linear increase in fatigue life. The scaling factor, a, was chosen so that the optimisation would be affected equally by a change in reflection coefficient or fatigue usage factor. The results of the optimisation process returned parameter values of $A = 1.6384$, $n = 2.4967$ and $m = 1.2502$, which have been used to produce the taper geometry definition illustrated graphically in Figures 5 and 7 in terms of both $M(x)$ and h_{mod} over the range of x and y for which the ABH taper is defined.

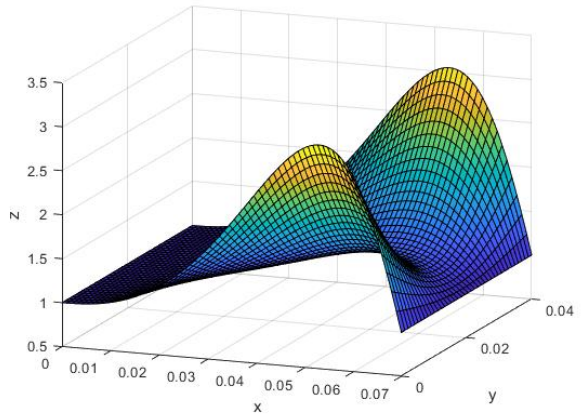

Figure 6: Equation 7 with parameter values of $A = 1.6384$, $n = 2.4967$ and $m = 1.2502$ plotted across the range of x and y over which the taper is defined.

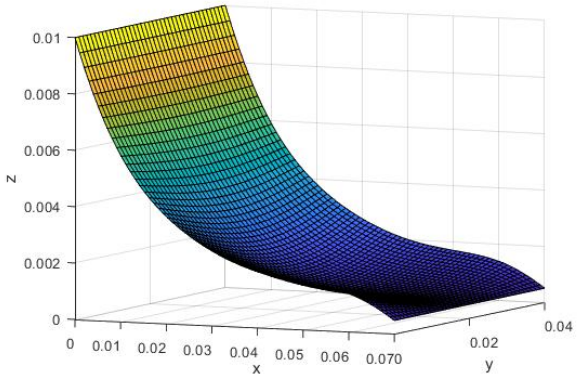

Figure 7: Modified taper profile for parameter values of $A = 1.6384$, $n = 2.4967$ and $m = 1.2502$.

The performance of the optimised modified profile is compared to the conventional profiles in Figure 5. For a direct comparison, the modified profile data point should be compared to the performance for a conventional ABH with a power law of 4, and this comparison shows that the modified profile gives a decrease in the maximum fatigue in the structure of around 10^2 with only a slight increase in the broadband averaged reflection coefficient. To provide further insight into the behaviour of the modified ABH taper design, Figure 8 shows the fatigue distribution for the modified profile. Comparing the results presented in Figures 4 and 8 it can also be seen that the modified profile has more noticeable concentrations at the edges of the structure, as well as the region of high fatigue occurring slightly closer to the ABH-beam junction in relation to the unmodified case. Nevertheless it is clear the proposed modified ABH taper design offers a potentially significant improvement in the fatigue life of the ABH taper without significantly compromising the vibration control performance.

6. CONCLUSIONS

ABHs are an effective and lightweight solution for the reduction of structural vibration, however, since they generally rely on decreasing the thickness of the structure there is a potential trade-off between vibration control performance and fatigue life. This paper has presented an investigation into the behaviour of an ABH taper beam termination, in terms of both its vibration attenuation performance and its fatigue life, before proposing a modified ABH profile that aims to reduce the effect of fatigue on the structure while maintaining the ABH effect.

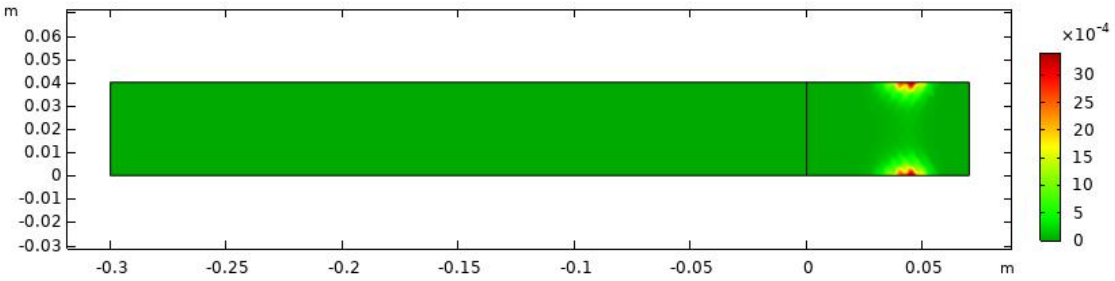

Figure 8: Fatigue usage factor across the surface of the beam and ABH for the modified profile.

The assessment of ABH performance in terms of both reflection and fatigue showed that ABHs are effective at reducing the reflections from the end of a beam, with the minimum broadband reflection coefficient being achieved for a power law of 4, but also show significant levels of fatigue in the ABH taper. For the considered structure, an input force of 20 N or above results in a fatigue life that is shorter than the required life expectancy of such a component, meaning that forces at this level would result in the ABH breaking prematurely. It was also shown throught the presented analysis, that the fatigue is concentrated at particular locations within the ABH taper. Based on this insight, a modification to the ABH profile has been proposed where the thickness of the structure is increased within the regions that exhibit high fatigue concentration in the conventional ABH design. The proposed modified profile is based on a mathematical function and the parameters of this function were optimised to reduce the fatigue without significantly impacting the performance in terms of the reflection coefficient. The resulting modified profile design is shown to provide a significant decrease in the maximum fatigue in the ABH with only a small increase in the broadband averaged reflection coefficient.

REFERENCES

[1] M A Mironov. Propagation of a flexural wave in a plate whose thickness decreases smoothly to zero in a finite interval. *(in English) Soviet Physics Acoustics - USSR*, 34(3):318–319, 1988.

[2] V V Krylov and F J B S Tilman. Acoustic 'black holes' for flexural waves as effective vibration dampers. *Journal of Sound and Vibration*, 274(3):605–619, 2004.

[3] K Hook, J Cheer, and S Daley. A parametric study of an acoustic black hole on a beam. *Journal of the Acoustical Society of America*, 145(6):3488–3498, 2019.

[4] P Feurtado and S Conlon. Investigation of boundary-taper reflection for acoustic black hole design. *Noise Control Engineering Journal*, 63(5):460–466, 2015.

[5] E. P. Bowyer and V. V. Krylov. Slots of power-law profile as acoustic black holes for flexural waves in metallic and composite plates. *Structures*, 6, 2016.

[6] D J O'Boy and V V Krylov. Vibration of a rectangular plate with a central power-law profiled groove by the rayleigh-ritz method. *Applied Acoustic*, 104:24–32, 2016.

[7] T Zhou, L L Tang, H L Ji, J H Qiu, and L Cheng. Dynamic and static properties of double-layered compound acoustic black hole structures. *International Journal of Applied Mechanics*, 9(5), 2017.

[8] M A Miner. cumulative damage in fatigue. *Journal of Applied Mechanics*, 12:A159–A164, 1945.

[9] P Strzelecki, A Correia, and J Sempruch. Estimation of fatigue s-n curves for aluminium based on tensile strength - proposed method. *MATEC Web of Conferences*, 338, 2021.

[10] A Karlos, S J Elliott, and J Cheer. Higher-order wkb analysis of reflection from tapered elastic wedges. *Journal of Sound and Vibration*, 449:368–388, 2019.

[11] C S Shin, K C Man, and C M Wang. A practical method to estimate the stress-concentration of notches. *International Journal of Fatigue*, 16(4):242–256, 1994.